Inorg. Chem. **2003**, *42*, 3509–3515

Structure and Magnetic Properties of the Two-Dimensional Ferrimagnet $(NEt_4)[\{Mn(salen)\}_2Fe(CN)_6]$: Investigation of Magnetic Anisotropy on a Single Crystal

Hitoshi Miyasaka,*[,†,‡] Hidenori Ieda,[§] Naohide Matsumoto,[||] Ken-ichi Sugiura,[†] and Masahiro Yamashita[†]

Department of Chemistry, Graduate School of Science, Tokyo Metropolitan University, and "Structural Ordering and Physical Properties," PRESTO, Japan Science and Technology Corporation (JST), 1-1 Minamiohsawa, Hachioji, Tokyo 192-0397, Japan, Department of Chemistry, Faculty of Science, Kyushu University, 6-10-1 Hakozaki, Higashi-ku, Fukuoka 812-8581, Japan, and Department of Chemistry, Faculty of Science, Kumamoto University, 2-39-1 Kurokami, Kumamoto 860-8555, Japan

Received December 12, 2002

The title compound, $(NEt_4)[\{Mn(salen)\}_2Fe(CN)_6]$ (**1**), was synthesized via a 1:1 reaction of $[Mn(salen)(H_2O)]ClO_4$ with $(NEt_4)_3[Fe(CN)_6]$ in a methanol/ethanol medium (NEt_4^+ = tetraethylammonium cation, $salen^{2-}$ = *N*,*N*′-ethylenebis(salicylidene)iminate). The two-dimensional layered structure of **1** was revealed by X-ray crystallographic analysis: **1** crystallizes in monoclinic space group $P2_1/c$ with cell dimensions of $a = 12.3660(8)$ Å, $b = 15.311(1)$ Å, $c = 12.918(1)$ Å, $\beta = 110.971(4)°$, $Z = 2$ and is isostructural to the previously synthesized compound, $(NEt_4)[\{Mn(5\text{-}Clsalen)\}_2Fe(CN)_6]$ (5-$Clsalen^{2-}$ = *N*,*N*′-ethylenebis(5-chlorosalicylidene)iminate; Miyasaka, H.; Matsumoto, N.; Re, N.; Gallo, E.; Floriani, C. *Inorg. Chem.* **1997**, *36*, 670). The Mn ion is surrounded by an equatorial salen quadridentate ligand and two axial nitrogen atoms from the $[Fe(CN)_6]^{3-}$ unit, the four Fe–CN groups of which coordinate to the Mn ions of $[Mn(salen)]^+$ units, forming a two-dimensional network having $[–Mn–NC–Fe–CN–]_4$ cyclic repeating units. The network is spread over the *bc*-plane of the unit cell, and the layers are stacked along the *a*-axis. The countercation NEt_4^+ is located between the layers. Compound **1** is a ferrimagnet with $T_c = 7.7$ K and exhibits hysteresis with a remnant magnetization of 13.44 $cm^3 \cdot mol^{-1}$ ($M/N\mu_B = 2.4$) at zero field and a coercivity of 1000 Oe when the powder sample was measured at 1.9 K. Magnetic measurements of a direction-arranged single crystal were also carried out. The orientation of the crystallographic axes of a selected single crystal was determined by X-ray analysis, and magnetization was measured when an external field was applied in the *a**, *b*, and *c* directions. The magnetization in the *a** direction increased more easily than those in the *b* and *c* directions below the critical temperature. No hysteresis was observed only for the measurement in the *a** direction, indicating the presence of strong structural anisotropy with potential anisotropy on Mn(III) ions.

Introduction

In the field of molecule-based magnetochemistry, polymer assemblies using hexacyano metalate $[M(CN)_6]^{3-}$ as a building component are an attractive research target because of their interests in bulk magnetism. The prussian-blue type compounds, $M_n[M(CN)_6]_m$, allowed various high-T_c three-dimensional (3-D) magnets[1−11] including room-temperature magnets ($T_c = 315$ K for $V^{II}_{0.42}V^{III}_{0.58}[Cr^{III}(CN)_6]_{0.86} \cdot 2.8H_2O$[10] and $Cs^{I}_{0.82}V^{II}_{0.66}[V^{IV}O]_{0.34}[Cr^{III}(CN)_6]_{0.92}(SO_4)_{0.203} \cdot 3.6H_2O$[11]), and molecular assemblies with coordination-acceptor metal complexes such as Ni(II) polyamine com-

* To whom correspondence should be addressed. E-mail: miyasaka@comp.metro-u.ac.jp.
† Tokyo Metropolitan University.
‡ PRESTO, JST.
§ Kyushu University.
|| Kumamoto University.

(1) Entley, W. R.; Girolami, G. S. *Science* **1995**, *268*, 397.
(2) Mallah, T.; Thiébault, S.; Verdaguer, M.; Veillet, P. *Science* **1993**, *262*, 1554.
(3) Grieber, W. D.; Babel, D. *Z. Naturforsch, B: Anorg. Chem., Org. Chem.* **1982**, *37*, 832.
(4) Gadet, V.; Mallah, T.; Castro, I.; Verdaguer, M. *J. Am. Chem. Soc.* **1992**, *114*, 9213.

10.1021/ic026261m CCC: $25.00
Published on Web 04/25/2003

plexes[12−16] and Mn(III) salen analogues[17] led to various magnetic materials exhibiting para-, ferro-, ferri-, or metamagnetism with their characteristic multidimensional architectures. We have directed our attention to magnetic materials including Mn(III) salen analogues. Our preliminary study on a family of two-dimensional (2-D) assemblies with Mn(III) salen analogues (SB), which is formally denoted by $A[\{Mn(SB)\}_2M(CN)_6]$ (A = monocation; M = Fe^{3+}, Mn^{3+}, Cr^{3+}, Co^{3+}), has increased our curiosity regarding magnetic anisotropy that crucially influences their bulk magnetism. In order to conduct detailed magnetic investigations such as single-crystal magnetic measurements to clarify anisotropic magnetism in low-dimensional materials, we prepared a new 2-D material, $(NEt_4)[\{Mn(salen)\}_2Fe(CN)_6]$ (**1**), in the form of well-shaped crystals. The compound is a member of the $A[\{Mn(SB)\}_2M(CN)_6]$ family and is similar to $(NEt_4)[\{Mn(5\text{-}Clsalen)\}_2Fe(CN)_6]$ in terms of structure and basic magnetism.[17e] Therefore, a detailed magnetic investigation of **1** is expected to offer a synthetic interpretation of the magnetism of the 2-D $A[\{Mn(SB)\}_2M(CN)_6]$ family. Herein, the structure and magnetic studies of both powder and single crystal samples of **1** are reported.

Experimental Section

General Materials. All chemicals and solvents used in the synthesis were of reagent grade. The parent materials of $[Mn(salen)(H_2O)]ClO_4$[18] and $(NEt_4)_3[Fe(CN)_6]$[19] were prepared according to methods in the literature, respectively. Perchlorate salts are potential explosives and should therefore be handled only in small quantities.

Preparation of 1. To a methanol solution (20 mL) of $[Mn(salen)(H_2O)]ClO_4$ (219 mg, 0.5 mmol) was added an ethanol solution (60 mL) of $(NEt_4)_3[Fe(CN)_6]$ (301 mg, 0.5 mmol) at room temperature. The resulting solution was filtered, and the filtrate was kept for 3 days in the dark at room temperature. Brown rhombic crystals that were formed were collected by suction filtration and washed with a small amount of ethanol. They were finally dried in vacuo (yield 86% for Mn). Anal. Calcd for $C_{46}H_{48}N_{11}O_4Mn_2Fe$: C, 56.11; H, 4.91; N, 15.65. Found: C, 56.04; H, 4.93; N, 15.49. IR (KBr pellet) (ν/cm^{-1}): 1601 (C═N), 1634 (C═N), 2106 (C≡N), 2131 (C≡N). Mp: >300 °C.

Physical Measurements. Infrared spectra were measured on a KBr disk with a Shimadzu FT-IR-8600 spectrophotometer. Magnetic susceptibility data were obtained over the temperature range 1.9−300 K at 0.1 T using an MPMS-XL SQUID susceptometer (Quantum Design, Inc.). Field dependencies of magnetization up to 7 T were studied on the same susceptometer. For magnetic measurements of a polycrystalline sample, the crystals were pulverized. On the other hand, for magnetic measurements of a single crystal of **1**, the axis orientation of the crystal was initially determined by X-ray analysis, and then, the crystal was arranged on a sample holder for magnetic measurements. For single-crystal magnetic measurements, an RSO SQUID attachment (Quantum Design, Inc.) was used for detecting very weak magnetization signals. Corrections were applied for diamagnetism using Pascal's constants[20] and for the sample holder.

X-ray Data Collection, Reduction, and Structure Determination. Measurement of **1** was conducted on a Rigaku imaging plate diffractometer (IP Rapid) with graphite monochromated Mo Kα radiation (λ = 0.71069 Å). Reflections (22076) were collected at −150 ± 1 °C, of which 5266 reflections were unique. The structure was solved by a direct method (SIR92)[21] and expanded using Fourier techniques.[17] The non-hydrogen atoms were refined anisotropically, whereas the hydrogen atoms were introduced as fixed contributors. Full-matrix least-squares refinements based on 4087 reflections with $I > 3.00\sigma(I)$ and reflection/parameter ratio = 12.61 were employed (unweighted and weighted agreement factors of $R1 = \sum||F_o| - |F_c||/\sum|F_o|$ and $R_w = [\sum w(F_o^2 - F_c^2)^2/\sum w(F_o^2)^2]^{1/2}$ were used). All calculations were performed using the teXsan crystallographic software package of Molecular Structure Corporation.[22] Crystal data and details of the structure determination for **1** are summarized in Table 1.

Results and Discussion

Synthesis and General Properties. Compound **1** was synthesized by the assembly reaction of $[Mn(salen)(H_2O)]ClO_4$ with $(NEt_4)_3[Fe(CN)_6]$ in a molar ratio of 1:1 in a methanol/ethanol medium. In contrast, the 1:1 reaction of

(5) Babel, D. *Comments Inorg. Chem.* **1986**, *5*, 285.
(6) Entley, W. R.; Girolami, G. S. *Inorg. Chem.* **1994**, *33*, 5165.
(7) Klenze, R.; Kanellakopoulos, B.; Trageser, G.; Eysel, H. H. *J. Chem. Phys.* **1980**, *72*, 5819.
(8) Herren, F.; Fischer, P.; Ludi, A.; Halg, W. *Inorg. Chem.* **1980**, *19*, 956.
(9) Gadet, V.; Bujoli-Doeuff, M.; Force, L.; Verdaguer, M.; Malkhi, K. E.; Deroy, A.; Besse, J. P.; Chappert, C.; Veillet, P.; Renard, J. P.; Beauvillain, P. In *Magnetic Molecular Materials*; Gatteschi, D., Kahn, O., Miller, J. S., Palacio, F. Eds.; NATO ASI Series E; Plenum: New York, 1991; Vol. 198.
(10) Ferlay, S.; Mallah, T.; Ouahés, R.; Vellet, P.; Verdaguer, M. *Nature* **1995**, *378*, 701.
(11) Dujardin, E.; Ferlay, S.; Phan, X.; Desplanches, C.; Cartier dit Moulin, C.; Sainctavit, P.; Baudelrt, F.; Dartyge, E.; Veillet, P.; Verdaguer, M. *J. Am. Chem. Soc.* **1998**, *120*, 11347.
(12) (a) Ohba, M.; Maruono, N.; Okawa, H.; Enoki, T.; Latour, J.-M. *J. Am. Chem. Soc.* **1994**, *116*, 11566. (b) Ohba, M.; Okawa, H.; Ito, T.; Ohto, A. *J. Chem. Soc., Chem. Commun.* **1995**, 1545. (c) Ohba, M.; Fukita, N.; Okawa, H. *J. Chem. Soc., Dalton Trans.* **1997**, 1733. (d) Ohba, M.; Okawa, H.; Fukita, N.; Hashimoto, Y. *J. Am. Chem. Soc.* **1997**, *119*, 1011. (e) Fukita, N.; Ohba, M.; Okawa, H.; Matsuda, K.; Iwamura, H. *Inorg. Chem.* **1998**, *37*, 842. (f) Ohba, M.; Usuki, N.; Fukita, N.; Okawa, H. *Inorg. Chem.* **1998**, *37*, 3349. (g) Ohba, M.; Usuki, N.; Fukita, N.; Okawa, H. *Angew. Chem., Int. Ed.* **1999**, *38*, 1795.
(13) Ferlay, S.; Mallah, T.; Vaissermann, J.; Bartolomé, F.; Veillet, P.; Verdaguer, M. *Chem. Commun.* **1996**, 2481.
(14) Fallah, M. S. E.; Rentshler, E.; Caneschi, A.; Sessoli, R.; Gatteschi, D. *Angew. Chem., Int. Ed. Engl.* **1996**, *35*, 1947.
(15) Langenberg, K. V.; Batten, S. R.; Berry, K. J.; Hockless, D. C. R.; Moubaraki, B.; Murray, K. *Inorg. Chem.* **1997**, *36*, 5006.
(16) Mallah, T.; Auberger, C.; Verdaguer, M.; Veillet, P. *J. Chem. Soc., Chem. Commun.* **1995**, 61.
(17) (a) Miyasaka, H.; Matsumoto, N.; Okawa, H.; Re, N.; Gallo, E.; Floriani, C. *Angew. Chem., Int. Ed. Engl.* **1995**, *34*, 1446. (b) Miyasaka, H.; Matsumoto, N.; Okawa, H.; Re, N.; Gallo, E.; Floriani, C. *J. Am. Chem. Soc.* **1996**, *118*, 981. (c) Re, N.; Gallo, E.; Floriani, C.; Miyasaka, H.; Matsumoto, N. *Inorg. Chem.* **1996**, *35*, 5964. (d) Re, N.; Gallo, E.; Floriani, C.; Miyasaka, H.; Matsumoto, N. *Inorg. Chem.* **1996**, *35*, 6004. (e) Miyasaka, H.; Matsumoto, N.; Re, N.; Gallo, E.; Floriani, C. *Inorg. Chem.* **1997**, *36*, 670. (f) Miyasaka, H.; Ieda, H.; Matsumoto, N.; Re, N.; Crescenzi, R.; Floriani, C. *Inorg. Chem.* **1998**, *37*, 255. (g) Miyasaka, H.; Okawa, H.; Miyazaki, A.; Enoki, T. *J. Chem. Soc., Dalton Trans.* **1998**, 3991. (h) Miyasaka, H.; Okawa, H.; Miyazaki, A.; Enoki, T. *Inorg. Chem.* **1998**, *37*, 4878. (i) Miyasaka, H.; Okawa, H.; Matsumoto, N. *Mol. Cryst. Liq. Cryst.* **1999**, *335*, 303.
(18) Shyu, H.-L.; Wei, H.-H.; Wang, Y. *Inorg. Chim. Acta* **1999**, *290*, 8.
(19) Mascharak, P. K. *Inorg. Chem.* **1986**, *25*, 245.
(20) Boudreaux, E. A.; Mulay, L. N. *Theory and Applications of Molecular Paramagnetism*; John Wiley and Sons: New York, 1976; pp 491−495.
(21) *SIR92*: Altomare, A.; Burla, M. C.; Camalli, M.; Cascarano, M.; Giacovazzo, C.; Guagliardi, A.; Polidori, G. *J. Appl. Crystallogr.* **1994**, *27*, 435.
(22) *teXsan: Crystal Structure Analysis Package*; Molecular Structure Corporation: The Woodlands, TX, 1985 and 1992.

Table 1. Crystallographic Information for **1**

formula	$C_{46}H_{48}N_{11}O_4Mn_2Fe$
fw	984.682
xpace group	$P2_1/c$ (No. 14)
T/°C	-150 ± 1
λ/Å	0.71069
a/Å	12.3660(8)
b/Å	15.311(1)
c/Å	12.918(1)
α/deg	90
β/deg	110.971(4)
γ/deg	90
V/Å^3	2283.8(3)
Z	2
D_{calcd}/g cm^{-3}	1.432
F_{000}	1018.00
μ(Mo Kα)/cm^{-1}	9.133
GOF	1.137
unique reflns	5266
no. obsd	4087 ($I > 3.00\sigma(I)$)
no. variables	324
R^a	0.058 ($I > 3.00\sigma(I)$)
$R_w{}^{b,c}$	0.170 ($I > 3.00\sigma(I)$)

[a] $R = \sum||F_o| - |F_c||/\sum|F_o|$ ($I > 3.00\sigma(I)$). [b] $R_w = [\sum w(F_o^2 - F_c^2)^2/\sum w(F_o^2)^2]^{1/2}$ ($I > 3.00\sigma(I)$). [c] $w = [\sigma_c^2(F_o^2) + (p(\max(F_o^2, 0) + 2F_c^2)/3)^2]^{-1}$ ($\sigma_c(F_o^2)$ = esd based on counting statistics; p = p-factor, 0.005 for **1**).

$[Mn(salen)(H_2O)]ClO_4$ with $K_3[Fe(CN)_6]$ in a methanol/water medium led to the formation of a hydrogen-bonded 3-D assembly, $[\{Mn(salen)\}_3\{Fe(CN)_6\}(H_2O)_2(MeOH)_2]\cdot 3H_2O\cdot$ MeOH, comprising four discrete hydrogen-bonding fragments of $[Mn(salen)(MeOH)Fe(CN)_6Mn(salen)(MeOH)]^-$, $[Mn_2(salen)_2(H_2O)_2]^{2+}$, $[Mn(salen)(H_2O)(MeOH)]^+$, and $[Fe(CN)_6]^{3-}$.[17b] Thus, the synthetic selectivity between these two compounds is in accord with the coordination ability of the cyanide nitrogen of $[Fe(CN)_6]^{3-}$ with $[Mn(salen)]^+$ species in competition with that of solvent pro-ligands and the packing effect in relation to the countercation of either NEt_4^+ or K^+. IR measurement of **1** revealed two C≡N vibrations at 2106 and 2131 cm^{-1}, in contrast to a single band at 2118 cm^{-1} for $(NEt_4)_3[Fe(CN)_6]$.

Structural Description. An ORTEP drawing of a formula unit of **1** is depicted in Figure 1 together with the atom numbering scheme. The relevant bond distances and angles are listed in Table 2. First, it should be noted that the overall structural feature of **1** is similar to those of the A[{Mn(SB)}$_2$M(CN)$_6$] family, particularly to that of $(NEt_4)[\{Mn(5\text{-}Clsalen)\}_2Fe(CN)_6]$;[17e] however, the magnetic behavior of some of the A[{Mn(SB)}$_2$M(CN)$_6$] family members is quite different from that of **1** in terms of the local exchange interaction between Mn and M ions and the interlayer interaction.[17] The trinuclear units of [Mn−NC−Fe−CN−Mn]$^-$ depicted in Figure 1 form a two-dimensional sheet using the four cyanide groups of $[Fe(CN)_6]^{3-}$ for binding $[Mn(salen)]^+$ units, as shown in Figure 2a. The geometry around the Mn(III) ion is assumed to be elongated octahedral with Jahn−Teller distortion in the direction of the [CN−Mn−NC] vector (Table 2). To form the network, two Mn−NC−Fe bonding modes are utilized: the bending mode [Mn1−N3−C17−Fe1] (Mn1−N3 = 2.266(3) Å and Mn1−N3−C17 = 167.8(3)°) and the relatively linear mode [Mn1−N4−C18−Fe1] (Mn1−N4 = 2.337(3) Å and Mn1−N4−C18 = 146.2(2)°). The bond distances and angles related to the two bonding modes are listed in Table 3, together with the corresponding parts of $(NEt_4)[\{Mn(5\text{-}Clsalen)\}_2Fe(CN)_6]$ and $[K\{Mn(3\text{-}MeOsalen)\}_2Fe(CN)_6]\cdot 2DMF$,[17a,b] the former of which and **1** have a ferrimagnetic 2-D network, whereas the latter has a ferromagnetic 2-D network. In this comparison, the two Mn−N bond distances of **1** are shorter than those of $[K\{Mn(3\text{-}MeOsalen)\}_2Fe(CN)_6]\cdot 2DMF$. A remarkable trend of the shorter Mn−N bond is also observed between $(NEt_4)[\{Mn(5\text{-}Clsalen)\}_2Fe(CN)_6]$ and $[K\{Mn(3\text{-}MeOsalen)\}_2Fe(CN)_6]\cdot 2DMF$. Although this structural aspect is expected to influence their magnetic behavior, it is difficult to gather definitive evidence from their structural features to explain the variety of local exchange coupling between these compounds.

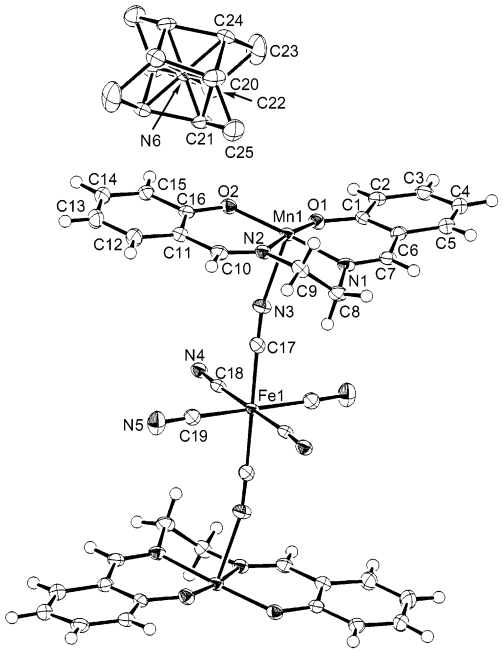

Figure 1. ORTEP drawing of a trinuclear structure and NEt_4^+ as the formula unit $(NEt_4)[\{Mn(salen)\}_2Fe(CN)_6]$ with the atom numbering scheme of the unique atoms (50% probability ellipsoids). Hydrogen atoms of the disordered NEt_4^+ are omitted for clarity.

Table 2. Relevant Bond Distances (Å) and Angles (deg) for $(NEt_4)[\{Mn(salen)\}_2Fe(CN)_6]$ (**1**) with the Estimated Standard Deviations in Parentheses

Fe1−C17	1.936(3)	C17−Fe1−C18	88.08(12)
Fe1−C18	1.945(3)	C17−Fe1−C19	91.91(13)
Fe1−C19	1.941(3)	C18−Fe1−C19	90.79(13)
Mn1−O1	1.888(2)	O1−Mn1−O2	94.86(9)
Mn1−O2	1.900(2)	O1−Mn1−N1	90.9(1)
Mn1−N1	1.997(3)	O2−Mn1−N1	174.20(9)
Mn1−N2	1.997(3)	O1−Mn1−N2	173.2(1)
Mn1−N3	2.266(3)	O2−Mn1−N2	91.9(1)
Mn1−N4*[a]	2.337(3)	N1−Mn1−N2	82.3(1)
N3−C17	1.154(4)	O1−Mn1−N	95.1(1)
N4−C18	1.168(4)	O2−Mn1−N3	92.5(1)
N5−C1	1.165(5)	N1−Mn1−N3	87.3(1)
		N2−Mn1−N3	83.9(1)
		O1−Mn1−N4*	91.97(9)
		O2−Mn1−N4	94.80(9)
		N1−Mn1−N4*	84.7(1)
		N2−Mn1−N4*	88.1(1)
		Mn1−N3−C1	167.8(3)
		Mn1−N4*−C18	146.2(2)

[a] Symmetry operations (*): $x, -y - 1/2, z - 1/2$.

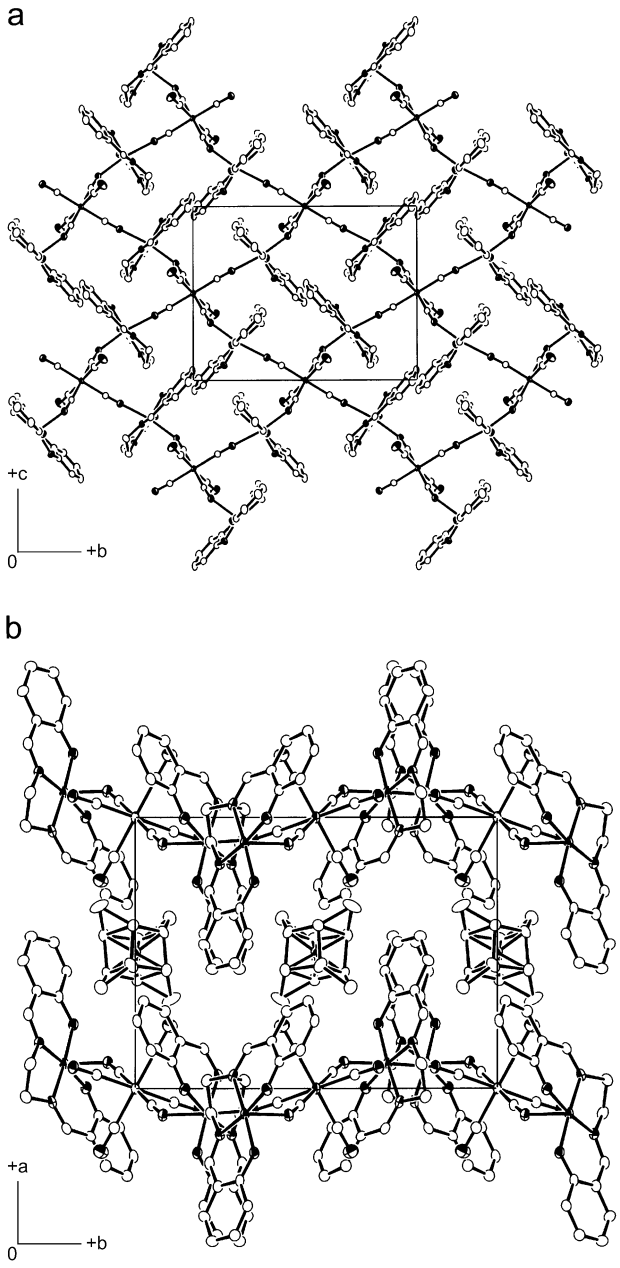

Figure 2. Packing diagrams of **1**, where Figure 2a shows a two-dimensional network projected along the *a*-axis of the unit cell, and Figure 2b shows a projection along the *c*-axis.

Table 3. Comparison of Relevant Bond Distances and Angles of the [−C(1)−N(1)-Mn−N(2)−C(2)−] Bonding Mode for **1**, (NEt_4)[{Mn(5-Clsalen)}$_2$Fe(CN)$_6$] (**2**), and [K{Mn(3-MeOsalen)}$_2$Fe(CN)$_6$]·2DMF (**3**)

	1	**2**	**3**
Mn−N(1)	2.266(3)	2.286(7)	2.290(5)
Mn−N(2)	2.337(3)	2.266(7)	2.415(5)
Mn−N(1)−C(1)	167.8(3)	154.4(7)	169.5(5)
Mn−N(2)−C(2)	146.2(2)	146.1(7)	137.2(4)

As shown in Figure 2a, the 2-D networks are spread over the *bc* plane of the unit cell; namely, the layer structure is stacked along the *a* axis, and the countercation NEt_4^+ is located between the 2-D Mn−Fe layers, as shown in Figure 2b.

Magnetic Consideration for the Powder Sample. The $\chi_m T$ versus T plot for the polycrystalline sample of **1** measured on a dc magnetosusceptometer is shown in Figure 3. The $\chi_m T$ value at room temperature is 6.68 cm^3·K·mol^{-1}, which is slightly larger than the value of 6.38 cm^3·K·mol^{-1} derived from a set of two high-spin Mn(III) $S_{Mn} = 2$ ions and one low spin Fe(III) $S_{Fe} = {}^1/_2$ ion assuming $g_{Mn} = g_{Fe} = 2.0$, even though it is sufficiently reasonable to expect that the Mn(III) ion has a slightly larger g_{Mn} value than 2.0. The $1/\chi_m$ value in the temperature range 20−300 K obeys the Curie−Weiss law with a negative Weiss constant of $\Theta = -2.8$ K and a Curie constant of $C = 6.69$ cm^3·K·mol^{-1}. Upon lowering the temperature, $\chi_m T$ decreases gradually to reach a minimum of 6.30 cm^3·K·mol^{-1} at 22 K, increases abruptly thereafter to reach a maximum of 62.7 cm^3·K·mol^{-1} at 7.0 K, and finally decreases again to 16.2 cm^3·K·mol^{-1} at 1.9 K. The decrease in the high-temperature region producing the negative Weiss constant and the presence of a minimum followed by an increase of $\chi_m T$ suggest that an antiferromagnetic coupling exists between high-spin Mn(III) ions and low-spin Fe(III) ions via CN^- bridging. As mentioned in the structural description, two Mn−NC−Fe bridging modes are present in the network. Although the magnitudes of the exchange interactions of the two modes are different, both modes should be antiferromagnetic, because of the sudden increase in what indicates a ferrimagnetic long-range order. If each exchange coupling were separately distinguishable as a combination of antiferromagnetic and ferromagnetic coupling, such a long-range order would not be expected, except when the spin canting system is assumed.

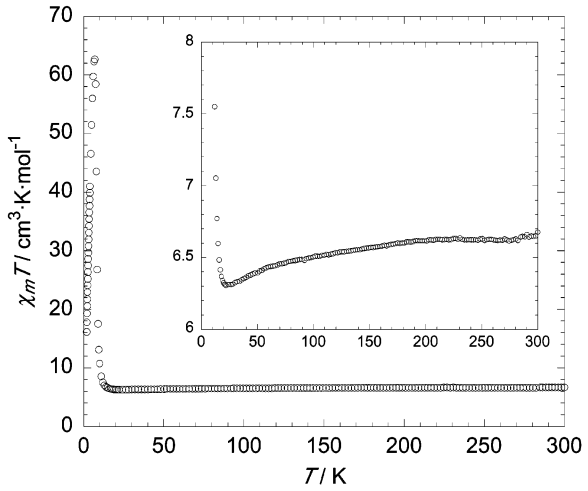

Figure 3. Temperature dependence of the $\chi_m T$ product at 1000 Oe measured on a polycrystalline sample of **1**.

Alternating current susceptibility of the polycrystalline sample was measured in the low-temperature region of 1.9−12 K at ac frequencies of 800, 1000, and 1200 Hz, as shown in Figure 4. Both in-phase χ' and out-of-phase χ'' signals were observed as a single sharp peak independent of the ac frequency. Both the maximum of χ' and the increasing χ'' were detected at almost the same temperature of 7.7 K, which could be attributed to a magnetic transition of a long-range order. Thus, the lack of dependence on frequency means that the transition is not due to random domain created by structural fluctuations and disordering.

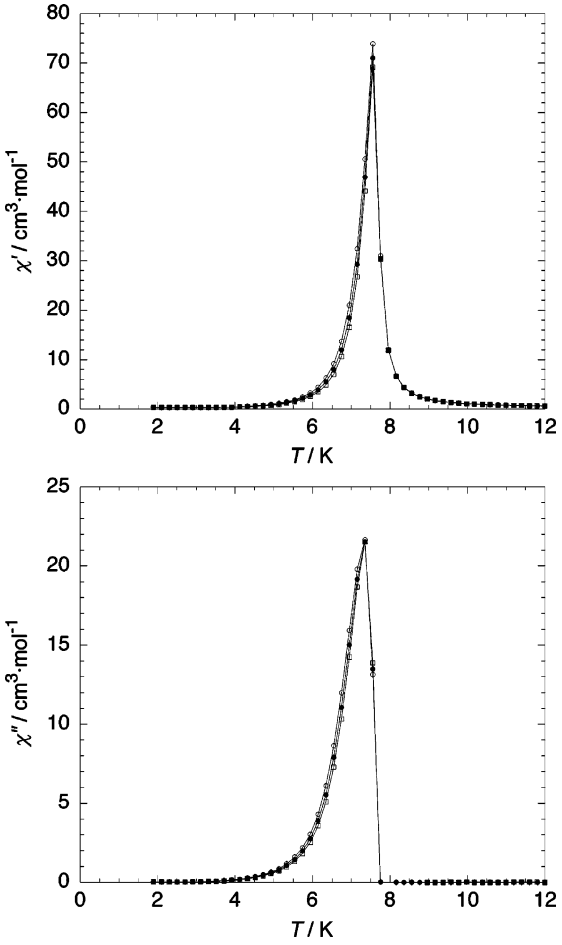

Figure 4. Temperature and frequency dependence of the (a) real (χ') and (b) imaginary (χ'') part of the ac susceptibility: ○, 800 Hz; ●, 1000 Hz; □, 1200 Hz. Solid lines are guides for eyes.

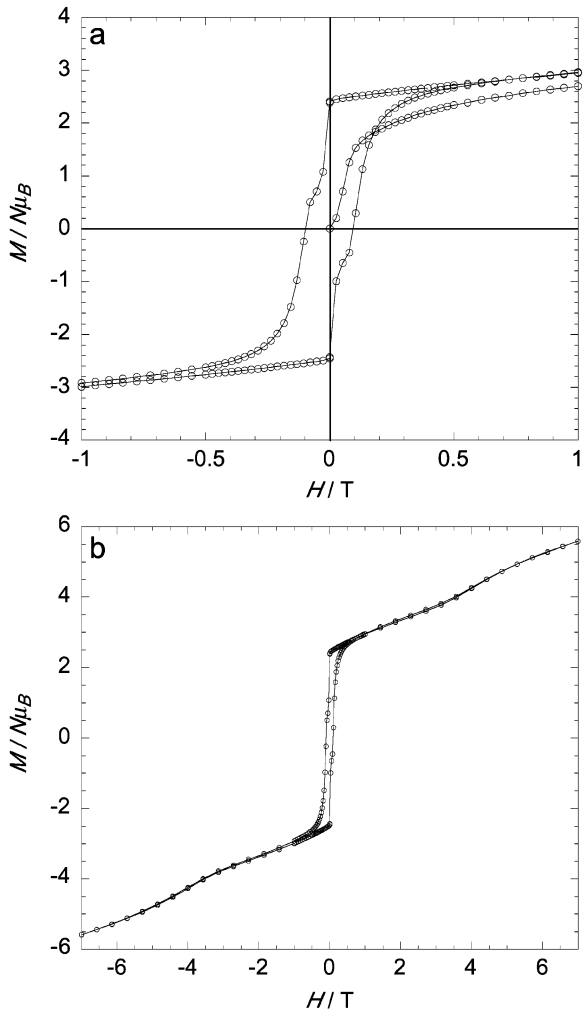

Figure 5. Hysteresis loop measured at 1.9 K of **1**. The solid lines are guides for eyes.

Measurement of magnetization vs external field at 1.9 K revealed a hysteresis, as shown in Figure 5. First, at low external magnetic fields, magnetization increases gradually with increasing external field and exhibits a small discontinuous point at approximately 200 Oe in an equivocal sigmoidal shape; then, it increases abruptly to $M/N\mu_B \approx 2$ under fields weaker than 1000 Oe. In the external field regions higher than 1 T, magnetization increases linearly to $M/N\mu_B = 5.6$ at 7 T. That value seems to be smaller than the expected value of $M/N\mu_B = 7$ assuming $g = 2$; however, that value and the increase in magnetization can be reasonably understood for this type of compound because of the presence of both magnetic anisotropy with the zero-field splitting effect in Mn(III) ions and structural anisotropy attributed to low dimensionality.[17b] Its capability as a magnet can be understood from the remnant magnetization of 13.44 $cm^3 \cdot mol^{-1}$ ($M/N\mu_B = 2.4$) at zero field and the coercivity of 1000 Oe, indicating a weak ferrimagnet. Note that the two modulating points at approximately zero field and 3 T are due to the influence of anisotropy arising from the structural low dimensionality of **1** (vide infra). Such modulation of the hysteresis was similarly observed for (NEt_4)[{Mn(5-Clsalen)}$_2$Fe(CN)$_6$] and [K{Mn(3-MeOsalen)}$_2$Fe(CN)$_6$]·2-DMF. Therefore, we performed magnetic measurements using a single crystal of **1** to obtain information about the magnetic anisotropy observed in the A[{Mn(SB)}$_2$Fe(CN)$_6$] family.

Single-Crystal Magnetic Measurements. For single-crystal magnetic measurements, a platelet single crystal having a size of $1.5 \times 1.0 \times 0.5$ mm^3 was selected, and prior to the measurements, the axis orientation of the crystal was determined by X-ray analysis. The temperature dependence of magnetization was measured in the temperature range 1.9−100 K under 1000 Oe. The $\chi_m T$ versus T and χ_m versus T plots are shown in Figure 6, where external magnetic fields are applied in three different directions, namely, a^*, b, and c directions (Figure 2). Both χ_m and $\chi_m T$ measured in the three directions increase abruptly in the temperature range 7−10 K, exhibiting long-range order of magnetic spins, but the data of $b//H$ show a smaller maximum value than the remaining two data. On the other hand, the largest maximum value was observed on $a^*//H$ measurement. Thus, the long-range order of magnetic spins is enhanced when the external magnetic field is applied perpendicularly to the 2-D Mn−Fe layers. This result confirms the presence of structural anisotropy derived from the three-dimensional structural packing in **1**, and the easy axis of magnetization corresponds to the a^* direction. When the external magnetic

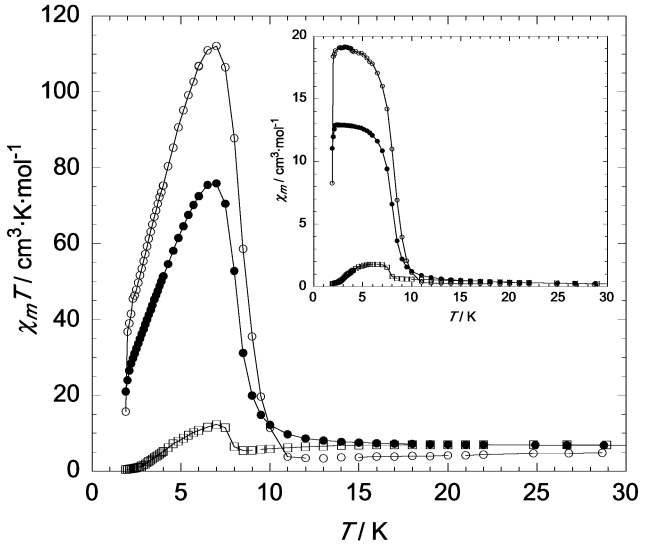

Figure 6. Temperature dependence of χ_m and $\chi_m T$ measured on a direction-arranged single crystal of **1** field-applied to *a**//*H* (○), *b*//*H* (□), and *c*//*H* (●), where the applied magnetic field is 1000 Oe.

field is applied in the *c* direction, being parallel to the 2-D Mn−Fe layers, the *c* direction allows relatively easy ordering of the magnetic spins compared to the *b* direction, although external field application in the *b* direction also allows spin ordering.

Field-dependence magnetization was measured while scanning the magnetic field from zero to 1 T, as shown in Figure 7a. As shown clearly, the three direction-arranged magnetizations are sigmoidal, probably due to the effect of anisotropy (vide infra). For the *a**//*H* direction, an abrupt increase in magnetization was observed at 600 Oe in the initial field scan, but after the second scan, this discontinuous feature was disappeared (Figure 7b).

Hysteresis loops were also measured in the magnetic field between −1 and +1 T for an arranged single crystal, as shown in Figure 7b. As expected from the *M* versus *T* data in Figure 6, the magnitude of the remnant magnetization follows the order *a**//*H* > *c*//*H* > *b*//*H*. In contrast, the magnitude of the coercivity is, interestingly, found to exhibit the reversed order, *a**//*H* < *c*//*H* < *b*//*H*, and particularly for the *a**//*H* measurement, no hysteresis is observed. This result may be related to the magnetic local anisotropy of the Mn(III) ions of $[Mn(salen)]^+$. As the Jahn−Teller axis of the $[Mn(salen)(NC-)_2]^+$ unit corresponds to the [CN−Mn−NC] vector of the out-of-plane of the $[Mn(salen)]^+$ molecule, the Jahn−Teller axis consequently lies on the 2-D sheets, thereby allowing a significant anisotropy. As mentioned already, the easy axis of the ordering magnetization of **1** locates perpendicular to the 2-D layers (*a** direction) and thus the Jahn−Teller axis. From this viewpoint, the effect of local anisotropy on Mn(III) ions is expected to be weak for spin ordering, but not negligible because it produces significant coercivity. Thus, the strong direction-dependent magnetic behavior may be produced by the two effects of structural anisotropy and local anisotropy contributed by the three-dimensional structural nature and the individual Mn(III) ions of $[Mn(salen)]^+$ units, respectively. Consequently,

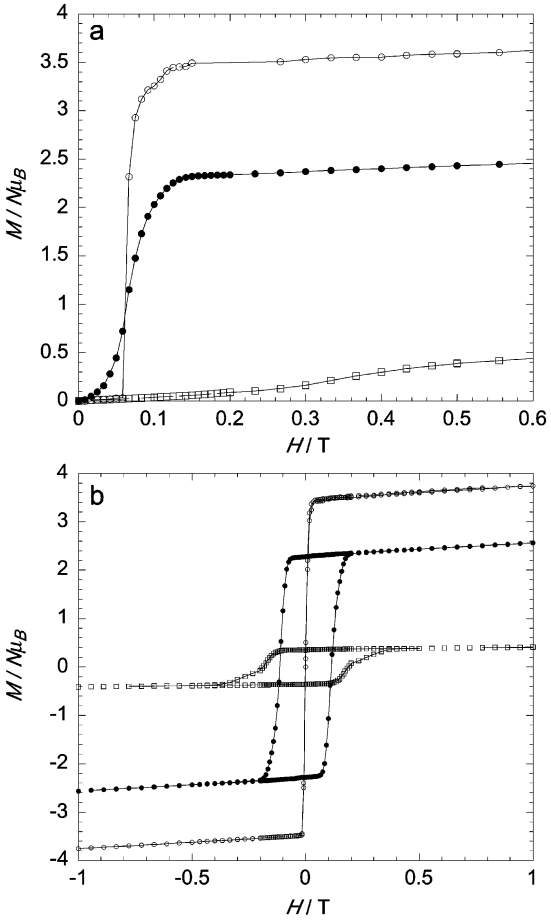

Figure 7. (a) Field dependence of the magnetization and (b) hysteresis loop at 1.9 K on a direction-arranged single crystal field-applied to *a**//*H* (○), *b*//*H* (□), and *c*//*H* (●).

the stepwise hysteresis observed on the polycrystalline sample may be understood as the influence of those anisotropies.

Conclusion

A 2-D layered compound, $(NEt_4)[\{Mn(salen)\}_2Fe(CN)_6]$, was discovered, and its magnetochemistry was studied in detail. The title compound is a ferrimagnet with $T_c = 7.7$ K. The total magnetic behavior of **1** is strongly affected by anisotropy arising from the low dimensionality of the structure (structural anisotropy) and the individual Mn(III) ions of $[Mn(salen)]^+$ units (local anisotropy). In our previous work, a similar magnetic behavior was observed in the series of $A[\{Mn(SB)\}_2Fe(CN)_6]$ (SB = salen analogues), as shown by a steplike hysteresis loop.[17b,e] Therefore, we conclude that the anisotropic magnetism of the $A[\{Mn(SB)\}_2Fe(CN)_6]$ family is almost identical to that of **1**. The anisotropic effects on molecule-based magnets possessing low-dimensional structures are one of the key points for understanding their bulk magnetism. One favored example is the work of Kahn et al., who reported the importance of anisotropy in the magnetostructural study of the two-dimensional cyano-bridged bimetallic compound, $K_2Mn_3(H_2O)_6[Mo(CN)_7]\cdot 6H_2O$.[23]

We intend to explore further the chemistry of assembled compounds including Mn(III) salen analogues. In particular,

low-dimensional compounds are very interesting because the control of magnetic anisotropy may open new doors to the chemistry and physics of magnetic materials. In fact, some high-spin clusters, the so-called *single-molecule magnets*,[24] and isolated one-dimensional chains, the so-called molecular magnetic nanowires or *single-chain magnets*,[25,26] have been reported in succession. For those materials, the specific magnetism is closely related to the anisotropy of the molecules themselves and the local anisotropy of the constituting metal centers. Investigations are underway to discover new materials in the Mn(III) salen assembly system.

Acknowledgment. This work was supported by a grant from PRESTO, Japan Science and Technology Corporation (JST) (H.M.), and a grant from Tokuyama Science and Technology Foundation (H.M.).

Supporting Information Available: X-ray crystallographic file in CIF format for the structural analysis of **1**. This material is available free of charge via the Internet at http://pubs.acs.org.

IC026261M

(23) Larionova, J.; Kahn, O.; Gohlen, S.; Ouahab, L.; Clérac, R. *J. Am. Chem. Soc.* **1999**, *121*, 3349.

(24) For example: (a) Sessoli, R.; Gatteschi, D.; Caneschi, A.; Novak, M. A. *Nature* **1993**, 365, 141. (b) Gatteschi, D.; Caneschi, A.; Pardi, L.; Sessoli, R. *Science* **1994**, 265, 1054. (c) Thomas, L.; Lionti, F.; Ballou, R.; Gatteschi, D.; Sessoli, R.; Barbara, B. *Nature* **1996**, 383, 145. (d) Ruiz, D.; Sun, Z.; Albela, B.; Folting, K.; Ribas, J.; Christou, G.; Hendrickson, D. N. *Angew. Chem., Int. Ed.* **1998**, *37*, 300.

(25) Caneschi, A.; Gatteschi, D.; Lalioti, N.; Sangregorio, C.; Sessoli, R.; Venturi, G.; Vindigni, A.; Rettori, A.; Pini, M. G.; Novak, M. A. *Angew. Chem., Int. Ed.* **2001**, *40*, 1760.

(26) Clérac, R.; Miyasaka, H.; Yamashita, M.; Coulon, C. *J. Am. Chem. Soc.* **2002**, *124*, 12837.